PCCP

Accepted Manuscript

ROYAL SOCIETY OF CHEMISTRY

www.rsc.org/pccp

Layered structure of croconic acid and radial distributions from large scale MD simulations, highlighting a distinct broadening even at 300K where the material remains ferroelectric.

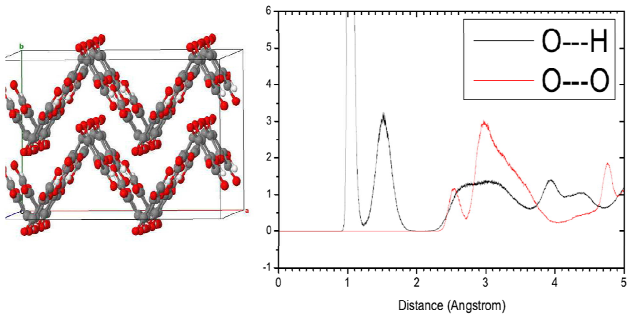

Hydrogen-bond Structure and Anharmonicity in Croconic Acid

Sanghamitra Mukhopadhyay,*[a,b] Matthias Gutmann,[a] and Felix Fernandez-Alonso[a,c]

Received Xth XXXXXXXXXX 20XX, Accepted Xth XXXXXXXXX 20XX
First published on the web Xth XXXXXXXXXX 200X
DOI: 10.1039/b000000x

First-principles molecular dynamics simulations and neutron-scattering experiments have been employed to investigate the structure and underlying vibrational motions in croconic acid as a function of temperature over the range 4-400K. Calculated hydroxyl-bond distances were within 4% of the experimentally determined bond lengths. Temperature-dependent structures have been explored using large-scale molecular dynamics simulations. From the calculated radial distribution functions, it is found that medium-range order associated with O···H and O···O correlations are affected by an increase in temperature, yet the characteristic long-range layered structure of this material remains unaltered. Hydrogen-bond anharmonicity has been assessed from the molecular dynamics simulations, showing a red shift of ca. 50 cm^{-1} of the O-H stretch frequency relative to quasi-harmonic results. This shift shows the importance of anharmonic corrections on hydrogen bonds in solid croconic acid.

Introduction

Crystalline croconic acid (CA),[1] molecular formula $C_5O_5H_2$, is an above-room-temperature ferroelectric. Although the size of the molecule in this molecular crystal is relatively small, it displays the highest-known bulk polarization for a carbon-based material (P$\sim$20 μC cm^{-2}) with low coercive field (11 kV/cm^{-1}). These features make its performance comparable to the best inorganic ferroelectrics such as barium titanate ($BaTiO_3$).[2] Ferroelectricity in CA remains almost constant in the temperature range 4-400 K, which is a remarkable phenomenon for a hydrogen-bonded molecular crystal. In this and previous works,[3,4] we seek to obtain an atomistic understanding of this organic ferroelectric material via the use of first-principles computational modelling in conjunction with experiment.

The structure and intermolecular forces of CA, including the position of the hydrogen ions, are important parameters to understand the mechanism of its ferroelectricity. The location of the hydrogen ions in CA had to await neutron scattering experiments.[3,4] Interatomic forces have been derived from vibrational assignments of matrix-isolated CA[5] using polarization-sensitive infrared (IR) spectroscopy and isolated-molecule ab initio calculations. In these calculations, hydrogen bonding between adjacent hydroxyl (OH) groups in CA is intrinsically of an intramolecular nature and, therefore, it does not reflect intermolecular interactions with the surrounding molecules. In the solid state, the chemical environment of crystalline CA has also been probed using nuclear magnetic resonance (NMR).[6] These experiments, using both ^{13}C and ^{17}O nuclear-quadrupole-resonance spectra, reveal the presence of five non-equivalent carbon sites and they are consistent with an OH bond length of 0.99$\pm$0.01 Å. This latter result agrees with neutron diffraction data where differences in length between two non-equivalent OH bonds in solid CA is found to be less than 1%.[3,4]

X-ray photoelectron spectroscopy (XPS) experiments and first-principles calculations on CA thin films have also provided important insights into hydrogen-bonding motifs in CA in the solid state.[7] From these experiments and parallel first-principles calculations, it has been concluded that the main difference between the isolated molecule and the crystal in terms of electronic structure occurs in the range 6-12 eV in the electronic density of state, where a doublet characteristic of solid CA is absent in the isolated molecule. In a similar vein, low-temperature vibrational data obtained from inelastic neutron scattering (INS) experiments complemented with first-principles simulations have also been reported. A prominent doublet at energy transfers around 900 cm^{-1} served to identify two distinct types of hydrogen bond in CA.

On the computational front, first-principles density-functional-theory (DFT) calculations have been reported using a number of approximations and functionals, including: the local density approximation (LDA); [1] the generalized gradient approximation (GGA)[8,9] as well as its Perdew-Burke-Ernzerhof (PBE) parametrization; [3,4,9] the Heyd-Scuseria-Ernzerhof (HSE) functional [9]; dispersion-corrected van der Waals functionals (PBE+D) following the methodology of Grimme[9] and Tkatchenko-Scheffler;[3,4] and projected-augmented wave (PAW) method with DFT-D2

0[a] *ISIS Facility, STFC Rutherford Appleton Laboratory, Didcot, Oxfordshire, OX11 0QX, UK. Fax: XX XXXX XXXX; Tel: +44(0)1235778190; E-mail: sanghamitra.mukhopadhyay@stfc.ac.uk*
0[b] *Imperial College London, Exhibition Road, London SW7 2AZ, UK.*
0[c] *University College London, Gower Street, London WC1E 6BT, UK.*

functional[10] on CA. From these calculations, it has been found that the consideration of van der Waals interactions as implemented with the PBE+D functional are important for a correct prediction of lattice constants; however, vibrational properties appear to be less sensitive to the particular choice of functional.[3,4]

To understand the nature of interatomic forces and hydrogen bonding in this material, first-principles calculations have been performed within the quasi-harmonic approximation, as well as using molecular-dynamics (MD) simulations within the framework of dispersion-corrected DFT. As a continuation of recent studies,[3,4] a detailed assessment of these results is also performed via direct comparison with temperature-dependent neutron-scattering data. We also make use of these MD simulations to explore the intermolecular forces associated with hydrogen bonding beyond the quasi-harmonic approximation, as well as how these departures may be related to the underlying structure and properties of CA in the solid state.

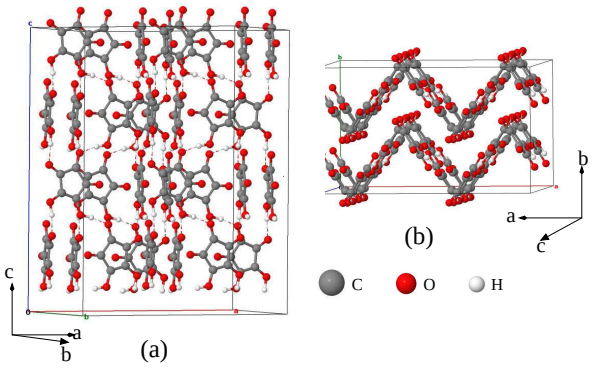

Fig. 1 The MD simulation cell structure of croconic acid, (a) front view (b) side view.

1 Methodology

Electronic-structure calculations were performed with plane-wave pseudopotentials as implemented in the CASTEP code.[11] In all calculations, optimized norm-conserving pseudopotentials[12] generated with the Perdew-Burke-Ernzerhof (PBE)[13] functional within the generalized-gradient approximation (GGA) have been used. Dispersion corrections to the PBE functional (PBE+D) were included following the methodology of Tkatchenko and Scheffler.[14,15] A plane-wave cutoff of 800 eV and a Brillouin-zone (BZ) sampling of 6x6x3 k-points (18 points when symmetry-reduced) were found to be sufficient to converge energy and atomic forces below $9.6\text{x}10^{-3}$ eV/ion and $1.0\text{x}10^{-3}$ eV/Å, respectively. Self-consistent single-point energy minimizations used a tolerance of $2.5\text{x}10^{-9}$ eV. Full-geometry optimizations were performed with a force tolerance of $1.0\text{x}10^{-3}$eV/Å using the Broyden-Fletcher-Goldfarb-Shanno (BFGS) algorithm. Temperature-dependent properties have been calculated within the quasi-harmonic approximations, where internal coordinates have been optimised on crystal structures with experimentally obtained lattice parameters.

Phonon frequencies and eigenvectors of the resulting minimum-energy structures were calculated via diagonalization of dynamical matrices computed using density-functional perturbation theory (DFPT) and linear-response methods.[16] In CASTEP, use of DFPT methods with dispersion-corrected functionals is not currently implemented and, therefore, only the PBE functional was used in these calculations. Using DFPT, phonon dispersion calculations were performed on a total of 8-q points followed by interpolation to obtain a total of 209 q-points within the BZ.

First-principles MD simulations have been performed on a $2 \times 2 \times 2$ supercell consisting of 384 atoms, i.e., 32 CA molecules, at a single **k** point with periodic boundary condition and plane-wave pseudopotentials as implemented in the CASTEP code.[11] The MD simulation cell considered for calculations is shown in Fig. 1. The same norm-conserving pseudopotential with PBE functionals discussed above have been used. The cut off energies and tolerance for self consistent energy minimisation have also been kept the same. The NVT ensemble with Nose-Hoover thermostat was used to stabilise the temperature, where cell volumes were kept fixed to experimental values. A MD time step of 0.5 fs was used all throughout. NVT ensemble temperatures were equilibrated for 2 ps, followed by NVE production runs of 12 ps. Using 500 processors at the UK high-performance computing facility HECToR, these calculations took about 5 days/ps .

From these production runs, radial distribution functions (RDFs) and densities of states (DOS) have been calculated from MD trajectories using the nMoldyn code [17]. The radial distribution function, $g_{i,j}(r)$, has been calculated via the following relation:

$$g_{i,j}(r) = n_{i,j}(r)/[\rho_j 4\pi r^2 dr] \quad (1)$$

where $g_{i,j}$ is the radial distribution function of species i and j, $n_{i,j}$ is the corresponding histogram, r is the distance between two species, dr is the histogram shell width, and ρ_j is the average density of species j. In the current calculations, dr is 1.0×10^{-3} Å. The DOS has been calculated by a Fourier-cosine transformation of the time-dependent velocity autocorrelation function (VACF), $C_{j,j}$:

$$C_{j,j}(t) = (1/3) < v_j(0)\dot{v}_j(t) > \quad (2)$$

where $v_j(t)$ is the velocity of the species j at time t. This calculated DOS is then weighted by the incoherent neutron-

Table 1 Relevant ND and calculated structural parameters for solid CA as a function of temperature. Distances are in Å. ND error bars are given in parentheses and expressed in units of 10^{-3} Å. For the calculated structural parameters, percent values in parentheses indicate deviation between ND and calculation. An entry in *italics* denote a smaller ND value relative to calculation. See text for details.

Parameters	Temperatures							
	10 K		100 K		200 K		300 K	
	ND	Calculated	ND	Calculated	ND	Calculated	ND	Calculated
O-H(H)	1.008 (± 1.4)	1.040 (3.2%)	1.008 (± 2.0)	1.0392 (3.1%)	0.997 (± 2.5)	1.0380 (4.1%)	1.000 (± 2.3)	1.0369 (3.7%)
O-H(T)	1.005 (± 2.4)	1.044 (3.9%)	1.005 (± 2.0)	1.0434 (3.8%)	1.010 (± 2.6)	1.0420 (3.2%)	1.002 (± 2.5)	1.0408 (3.9%)
O··· H(H)	1.604 (± 1.4)	1.476 (*8.0%*)	1.604 (± 1.9)	1.4799 (*7.7%*)	1.617 (± 2.5)	1.4865 (*8.1%*)	1.631 (± 2.4)	1.4930 (*8.5%*)
O··· H(T)	1.611 (± 1.4)	1.531 (*5.0%*)	1.611 (± 2.1)	1.5400 (*4.4%*)	1.619 (± 2.6)	1.5406 (*4.8%*)	1.639 (± 2.3)	1.5473 (*5.6%*)
O···O(H)	2.594 (± 1.1)	2.517 (*3.0%*)	2.599 (± 1.7)	2.5204 (*3.0%*)	2.601(± 2.5)	2.5255 (*2.9%*)	2.617 (± 2.1)	2.5305 (*3.3%*)
O···O(T)	2.612 (± 1.1)	2.553 (*2.2%*)	2.610 (± 1.7)	2.5555 (*2.1%*)	2.622 (± 2.5)	2.5610 (*2.3%*)	2.633 (± 2.1)	2.5665 (*2.5%*)

scattering cross section of each species for comparison with the INS data.

Following the recipe of Braga et al.,[18] single crystals of CA have been grown in an inert helium atmosphere using commercially available powders (Sigma Aldrich No. 391700, 98% purity). Successive crystallization runs were carried out over a period of several weeks by slow evaporation in order to obtain well-defined (mm-sized) platelets. Neutron-scattering measurements were all performed at the ISIS Pulsed Neutron and Muon Source.[19] Temperature dependent single-crystal neutron diffraction (ND) measurements were performed on the SXD diffractometer[20] at selected temperatures, followed by a more detailed temperature study on the IRIS spectrometer using powder specimens and over the range $4-300$ K, where lattice parameters were determined following usual Rietveld profile refinement technique used for refinement of powder diffraction pattern. .[21] IRIS is an indirect-geometry low-energy spectrometer, which can also be used as a diffractometer in backscattering geometry. In this geometry, its resolution amounts to $\Delta d/d = 2.5\times10^{-3}$, where Δd is the resolution in d-spacing d . INS experiments were carried out on the TOSCA spectrometer at cryogenic temperatures (T<20K).[22]

2 Results and Discussion

CA is a hydrogen-bonded molecular crystal where pentagonal molecular units are arranged into planar sheets connected by hydrogen bonds as shown in Fig. 1. These sheets extend indefinitely along the crystallographic c-axis and adopt an accordion-like zig zag pattern making angles of about 45^0 with the $a-b$ plane. Two distinct types of hydrogen ions have been identified in previous INS studies,[3,4] so-called 'hinge' (along the c-axis, hereafter 'H'), and 'terrace' (on the a-b plane, hereafter 'T'). For a given CA molecule, one side of the pentagon is populated by two neighbouring hydroxyl (OH) group. The two oxygen atoms opposite to these OH groups within the same ring act as hydrogen-bond acceptors. The carbonyl (C=O) group sitting at the apex position of each pentagonal ring does not participate in hydrogen bonding.

ND patterns measured on IRIS at 4 and 300 K and associated fits are shown in Fig. 2. Bragg reflections have been indexed using the more detailed crystallographic data obtained on SXD. On the basis of these assignments, it becomes possible to fit the IRIS data so as to obtain cell parameters as a function of temperature. In all cases, ND data were refined within the non-centrosymmetric space group $Pca2_1$. A summary of the structural parameters relevant to the present work are given in Table 1.

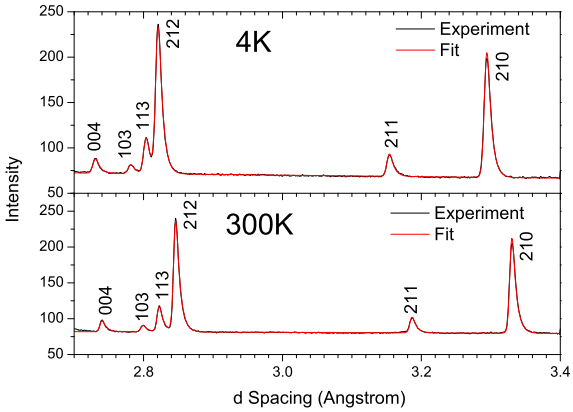

Fig. 2 ND patterns (black) and associated fits (red) obtained on IRIS at two selected temperatures. The numbers on the figure denote (*hkl*) reflections.

In Table 1, bond lengths and interatomic distances obtained from the first-principles simulations are compared with experiment. Given their putative relevance in explaining ferroelectric behaviour in CA,[3,4] we pay special attention to bond lengths related to the hydrogen atoms and interatomic distances between nearest-neighbour oxygen atoms. It is reassuring that calculated O-H bond lengths and O···O distances are within 4% of

experimental values. O···H(H) distances are a notable exception to the above, where differences are as high as 8%, particularly along the *c*-axis. On the basis of our PBE results, these larger deviations can be traced back to the nature of the van-der-Waals functional considered here, given its well-known tendency to overbind hydrogen bonds.[23] Likewise, the observed underestimation of hydroxyl-bond lengths and overestimation of hydrogen-bond lengths indicate that, irrespective of temperature, the calculated structure is less polar than the experimental one. Calculated lattice parameters (not reported here), also are within 3% of those measured at 4K[3,4] and within 2% of previous DFT studies by other authors.[9]

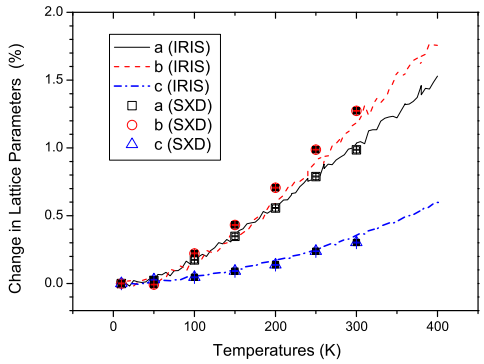

Fig. 3 Change in lattice parameters in CA measured on IRIS and SXD. Error bars in the SXD data are commensurate with the size of the symbols shown in the figure.

The dependence of lattice parameters with temperature obtained from the ND experiments are shown in Fig. 3. From this Figure and Table 1, it is found that all lattice constants increase monotonically with temperature. The relative increase along the *a* and *b* directions is larger than along the *c*-axis, indicating that the CA terraces (which are tilted at 45^o relative to the *a* or *b* directions), are widening with temperature. The increase in lattice parameters is, however, below 2% for temperatures up to 400 K. This finding is consistent with the absence of phase changes in CA up to its decomposition temperature, as previously reported by Horiuchi et al.[1]

The temperature dependence of bond lengths and relevant interatomic distances obtained from first-principles calculations are shown in Fig. 4. An increase in temperature translates into a shortening/lengthening of hydroxyl/hydrogen bonds. The O···O distance also increases with temperature, although such an increase remains below 1% up to 400 K. This trend indicates a progressive decoupling of individual CA molecules in the lattice with temperature, as a result of weaker intermolecular interactions, hydrogen bonding being the most prominent.

First-principles MD simulations provide further insight into

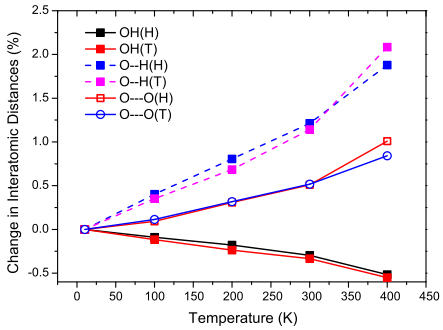

Fig. 4 Change in bond distances with temperature from first-principles calculations.

the effect of temperature on long-range structural parameters. Figures 5(a) and (b) show calculated RDFs for O···H, and O···O distances at 4 and 300 K, respectively.

As shown in inset of Fig. 5(a), long-range order associated with both O···H and O···O distances is evident at 4 K. The peak at 1.04 Å corresponds to hydroxyl (O-H) bonds and the next peak centred at 1.5 Å corresponds to O···H hydrogen bonds. The positional difference between O-H(T) and O-H(H) hydroxyl bonds cannot be distinguished from these data. These two different hydrogen bonds give rise to additional broadening of the aforementioned feature at 1.5 Å. A similar behaviour is also seen for O···O distances around 2.5 Å, corresponding to oxygen acceptor-donor pairs.

O···O distances around 3.0 Å and 3.5 Å are mainly of an intramolecular and intermolecular nature, respectively. Intermolecular O···O distances around 3.5 Å correspond to molecules in two adjacent terraces on next-neighbour sheets, whereas distances around 4.1 Å correspond to molecules in consecutive terraces separated by a chain of H hydrogen atoms. The sharp peak at 4.7 Å can be assigned to intramolecular O···O distances between the lone (not H-bonded) oxygen at the apex position of the pentagonal ring and oxygen furthest away within the same molecule.

To facilitate the discussion that follows, we define nearest-neighbour interatomic as well as intramolecular distances as short range, next-nearest neighbour intermolecular distances as medium range, and interplanar as long range. With these conventions in mind, short-range order in crystalline CA corresponds to hydrogen, hydroxyl, and O···O distances between nearest-neighbour molecular units. Long-range order, on the other hand, maps onto the relative arrangement of molecular units in different pleated sheets. Although these two types of order involve both hydrogen and oxygen, structural differences between short-range and long-range order for O···O pairs is clearly more prominent in the crystal structure of CA.

At 300K, as shown in Fig. 5(b), all peaks broaden. This

2 RESULTS AND DISCUSSION

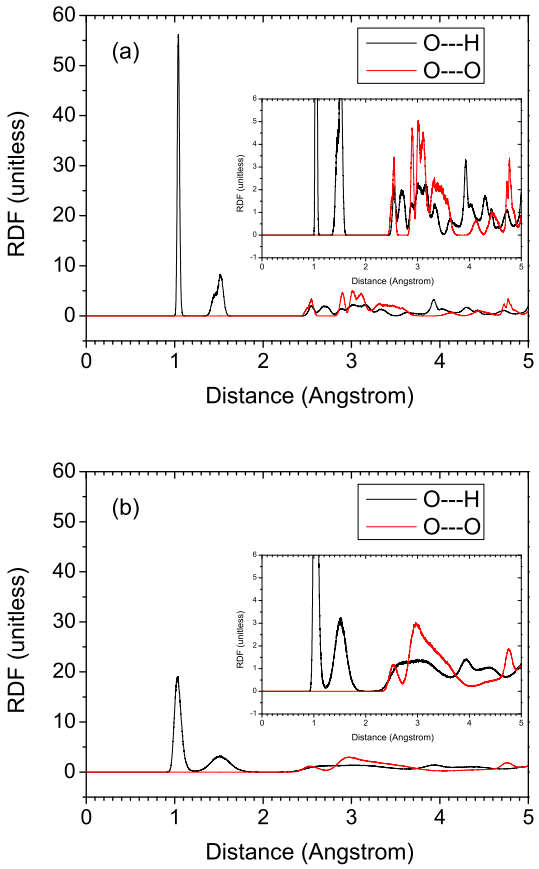

Fig. 5 RDFs for CA from first-principles MD simulations at (a) 4K and (b) 300K. RDFs around unity are shown in respective insets.

effect is more pronounced for the hydrogen-bond feature at 1.5 Å relative to the behaviour of the hydroxyl bond. Peaks corresponding to O···O distances also broaden considerably to the point they start merging with features associated with intramolecular O···O distances. No distinct signature is found in the RDF for H vs. T hydrogen atoms. This result shows that although there is no phase change due to an increase in temperature, the spatial distribution of hydroxyl and hydrogen bonds changes considerably due to thermally activated motions associated with both hydrogen and oxygen atoms. The broad distributions seen at intermediate distances arise from an increased flexibility of molecular units while keeping the basic layered structure unaffected. Hydrogen- and hydroxyl-bonds, which are surmised to play a key role in the ferroelectric properties of this material,[4] remain centred at the same lengths irrespective of temperature.

Signatures of long-range order are also found in O···O distances. O···O distances corresponding to distinct molecular units give rise to a broad peak where individual contribution from different oxygen atoms cannot be distinguished from each other. Features associated with distinct sheets (around 3.5 Å and 4.7 Å) are also prominent and display long-range order even at 300K. As stated above, this result indicates that the underlying pleated structure of this crystal remains unaffected with temperature. Nonetheless, significant structural changes happen for individual molecular units. Within the limitation of small cell size and simulation time, current calculations indicate that both short-range and long-range order are quite insensitive to temperature.

In the time window of the MD simulations, no proton transfer has been found even at 300 K, although proton transfer has been reported within 100 fs simulation time in two dimensional CA sheet using similar kind of MD simulations.[10] This result indicates that proton transfer in bulk CA does not appear to be mediated by temperature. On physical grounds, it is unlikely that the characteristic time for this transfer process is longer than our simulation time of 12 ps. Other mechanisms that could be at play and should be investigated further include the effects of external fields, and point or line defects in the layered structure.

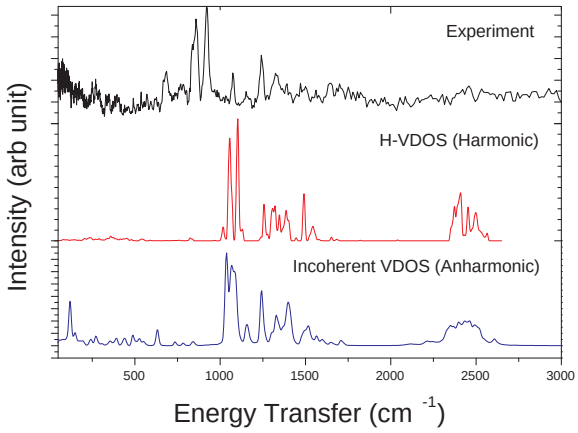

Fig. 6 INS spectrum and VDOS of CA at 5K. *Upper panel*: experimental INS spectrum; *middle panel*: hydrogen-projected VDOS from quasi-harmonic calculations; *lower panel:* incoherent VDOS from MD simulations.

INS experiments also enable us to to investigate the influence of these temperature-dependent structural changes on interatomic forces. To this end, the INS spectrum of CA is shown in the upper panel of Fig. 6. The hydrogen-projected vibrational DOS (VDOS) calculated within the quasiharmonic and anharmonic approximations are shown in the middle and lower panels, respectively, of the same figure. The doublet at 1056 cm^{-1} and 1110 cm^{-1} in the quasiharmonic VDOS corre-

sponds to out-of plane bending motions of two hydrogen ions, as discussed in our earlier reports[3,4]. Difference in the calculated and experimental vibrational frequencies for these intermolecular O···-H-O bending modes in the quasiharmonic approximation is about 15%. Referring back to Fig. 3, it becomes apparent that the observed lattice expansion arises from additional (anharmonic) contributions to the interatomic potential.[24] To assess these effects in more detail, the MD simulations have been used to calculate classical VDOS beyond the harmonic and quasiharmonic approximations, as shown in the lower panel of Fig. 6. The two bend modes described above are red shifted by about 30 cm^{-1}. The accompanying shift in stretch frequencies (around 2500 cm^{-1}) due to anharmonicity is about 50 cm^{-1}. The VDOS of isolated CA molecule have been compared with that of solid state by us [3] previously. The comparison shows that C=O stretching modes are red-shifted by 13% in the solid state CA. That shift reduces to below 1% when anharmonicity is considered in both calculations.

Noting that the anharmonic shift of the O-H···O bending mode in water is 40 cm^{-1} [25] and that the OH stretching mode is 83 cm^{-1},[26] our results show that anharmonic corrections in CA are of a similar magnitude at similar frequencies. In comparison with the INS data, vibrational frequencies are still overestimated by about 14% even if anharmonicity is considered. Finite-size effects of the simulation cell used for the MD calculations could be one source of error, as mentioned earlier.[27] Other important factors include the nuclear quantum motion of the hydrogen atoms in solid CA. These latter calculations, while interesting in their own right, are beyond the scope of the current study. In spite of these limitations, this work is a step forward to understand hydrogen bonding in solid CA showing the importance of anharmonic corrections on O-H potential.

3 Conclusions

In this paper, we have presented temperature-dependent ND data and first-principles DFT calculations on solid CA over a wide temperature range (4-400 K). The effects of temperature on the structure of this organic material have been explored within the quasiharmonic approximation as well as via large-scale MD. Overall, calculated interatomic distances were within 4% of experimental values. From calculated RDFs, it is found that temperature has a clear effect on the medium-range order associated with O-H and O···O distances, yet at the same time long-range order remains largely undisturbed. This finding imply an increased flexibility of molecular units as a function of temperature while the basic layered structure remains unaffected. Anharmonic corrections to hydrogen-bond motions are also found to be significant and of a similar magnitude to what is characteristic of other hydrogen-bonded systems. The doublet observed in the INS experiments near 900 cm^{-1} are red shifted by 30 cm^{-1} due to the anharmonic nature of the vibration of the hydrogen-bonds bending mode. OH stretching frequencies are also shifted by an average of 50 cm^{-1}. This work is a step forward to understand hydrogen bonding in solid CA showing the importance of anharmonic corrections on O-H potential.

Acknowledgements

Authors would like to thank Keith Refson, Dominik Jochym, and Simone Sturniolo for many useful discussions. We thank the ISIS Facility for the provision of beam time, and the UK Science and Technology Facilities Council e-Science Department for continued access to the SCARF cluster at the Rutherford Appleton Laboratory. Some of the computations have been performed on the UK High Performance Computing Facility HECToR under the auspices of the Materials Chemistry Consortium (EPSRC grant EP/D504872).

References

1 S. Horiouchi, Y. Tokunaga, G. Giovannetti, S. Picozzi, H. Itoh, R. Shimano, R. Kumai and Y. Tokura, *Nature*, 2010, **463**, 789.

2 K. Rebe, C. H. Ahn and J. M. T. E.), *Physics of Ferroelectrics: A Modern Perspective*, Spinger-Verlag Berlin Heidelberg, 2007.

3 F. Fernandez-Alonso, M. J. Gutmann, S. Mukhopadhyay, D. B. Jochym, K. Refson, M. Jura, M. Krzystyniak, M. Jimenez-Ruiz and A. Wagner, *J. Phys. Soc. Japan*, 2013, **82**, SA001.

4 S. Mukhopadhyay, M. J. Gutmann, M. Jura, D. B. Jochym, M. Jimenez-Ruiz, S. Sturniolo, K. Refson and F. Fernandez-Alonso, *Chem Phys*, 2013, **427**, 95.

5 T. Kolev, B. B. Koleva and M. Spiteller, *Cent. Eur. J. Chem.*, 2008, **6**, 393.

6 J. Seliger, J. Plavec, P. Sket, V. Zagar and R. Blinc, *Phys. Status Solidi B*, 2011, **248**, 2091.

7 F. Bisti, A. Stroppa, S. Picozzi and L. Ottaviano, *J. Chem. Phys*, 2011, **134**, 174505.

8 A. Stroppa, D. D. Sante, S. Horiuchi, Y. Tokura, D. Vanderbilt and S. Picozzi, *Phys. Rev. B*, 2011, **84**, 014101.

9 D. D. Sante, A. Stroppa and S. Picozzi, *Phys. Chem. Chem. Phys*, 2012, **14**, 14673.

10 D. A. Kunkel, J. Hooper, S. Simpson, G. A. Rojas, S. Ducharme, T. Usher, E. Zurek and A. Enders, *Phys. Rev. B*, 2013, **87**, 041402(R).

11 S. J.Clark, M. Segall, C. J. Pickard, P. J.Hasnip, M. J. Probert, K.Refson and M. Payne, *Z Kristallogr*, 2005, **220**, 567.

12 A. M. Rappe, K. M. Rabe, E. Kaxiras and J. D. Joannopoulos, *Phys. Rev. B*, 1990, **41**, 1227.

13 J. P. Perdew, K. Burke and M. Ernzerhof, *Phys. Rev. Lett.*, 1996, **77**, 3865.

14 A. Tkatchenko and M. Scheffler, *Phys. Rev. Lett..*, 2009, **102**, 073005.

15 E. R. McNellis, J. Meyer and K. Reuter, *Phys. Rev. B*, 2009, **80**, 205414.

16 K. Refson, S. J. Clark and P. R. Tulip, *Phys. Rev. B*, 2006, **73**, 155114.

17 G. R. Kneller, V. Keiner, M. Kneller and M. Schiller, *Comput. Phys. Comm.*, 1995, **91**, 191.

18 D. Braga, L. Maini, and F. Grepioni, *Cryst. Eng. Comm*, 2001, **6**, 1.

19 *http://www.isis.stfc.ac.uk/*, 2014, 10 April.

20 *http://www.isis.stfc.ac.uk/instruments/sxd/*, 2013, 15 June.

21 *http://www.isis.stfc.ac.uk/instruments/iris/*, 2014, 10 April.

22 *http://www.isis.stfc.ac.uk/instruments/tosca/*, 2014, 10 April.

23 G. A. Jeffrey, *An Introduction to Hydrogen Bonding*, Oxford University Press, 1997.

24 B. Monserrat, N. D. Drummond and R. J. Needs, *Phys Rev B*, 2013, **87**, 144307.

25 T. D. Fridgen, T. B. McMahon, L. MacAleese, J. Lemaire and P. Maitre, *J. Phys. Chem. A*, 2004, **108**, 9008.

26 G. Herzberg, *Molecular Spectra and Molecular Structure*, Krieger Publishing Company, 1989.

27 O. Hellman, I. A. Abrikosov and S. I. Simak, *Phys. Rev. B.*, 2011, **84**, 180301(R).